A COMPLETE TOOLBOX FOR ABDOMINAL SOUNDS SIGNAL PROCESSING AND ANALYSIS

R. Ranta*, V. Louis-Dorr*, Ch. Heinrich**, D. Wolf* and F. Guillemin***

* Institut National Polytechnique de Lorraine /
CRAN UMR INPL-UHP-CNRS 7039,Vandoeuvre-lès-Nancy, France
** Laboratoire des Sciences de l'Image, de l' Informatique et de la Télédétection /
LSIIT UMR ULP-CNRS 7005, Illkirch, France
*** Centre Alexis Vautrin /
CRAN UMR INPL-UHP-CNRS 7039, Vandoeuvre-lès-Nancy, France

radu.ranta@ensem.inpl-nancy.fr

Abstract: The general framework of this communication is phonoenterography. Our objective is the development of a non-invasive medical exploratory tool contributing to the functional study of the gastro-intestinal physiology. Abdominal sounds are studied for more than a century, but the results are rather poor and sometimes contradictory [1–7]. Our main hypothesis is that abdominal sounds, recorded upon long periods of time and using several stethoscopes, are useful for medical interpretation of the underlying physiological activity, either normal or pathologic. In order to check this hypothesis, we have developed a complete signal processing and analysis toolbox, described in the following section. Parts of this work have been presented in [8–11]. This communication presents the complete processing chain and introduces new features added to the pre-processing step. Data analysis is performed on a larger data base of abdominal sounds, recorded on healthy volunteers.

Introduction

One of the oldest means of physiological investigation, still currently used in clinical routine, is the auscultation. The instrumentation is simple (stethoscope) and its utility is largely recognized especially for cardiac and pulmonary sounds, but also for abdominal and fetal sounds. Relatively little studied for the abdominal physiological sounds (although the first papers appeared a century ago [1]), it presents significant potentialities because these sounds are rich in information [1–6, 12]. Still, medical conclusions remain very few. In fact, abdominal auscultation interpretation is particulary difficult, mainly because of the sounds highly irregular character, their random appearance, their inter-patient variability and finally, because of the necessity of a long duration auscultation.

It is then interesting to develop an automatic tool for clinical diagnosis and medical research, based on the systematic long-term recording and processing of the abdominal sounds. One can assume that abdominal sounds are an indication for the motor activity of the various segments of the gastro-intestinal tract: during digestion, the bolus is transformed and transported along the digestive tract, causing noises. Different application can be imagined, from the study of the normal physiology to clinical routine (functional diseases diagnostic aid, post-surgical monitoring) or pharmacological research (medication effect on the gastro-intestinal activity).

The goal of our research is the construction of a "toolbox" dedicated to the phonoenterogram processing, capable to provide medical interpretable data (i.e to distinguish various operating modes of the digestive tract). This leads to a classical bio-medical signal processing approach, involving several aspects presented in the next section of this communication:

- The **instrumentation** must allow a faithful recording of the signals of interest, while minimizing the incidence of the interfering signals. It must be robust to possible changes in clinical conditions and it must facilitate the medical validation, which is the "golden standard" of all bio-medical research;
- The **preprocessing** of the acquired signals must transform the rough signal into an interpretable one by denoising, segmentation and localization. As parts of this work have been presented in [8, 9], we will insist here on a new method of denoising and segmentation, which takes into account local dynamics of the non-stationary explosive bowel sounds;
- One of the novelties of our approach is the **multichannel** parallel recording and processing of abdominal sounds, permitting approximate localization of the sounds source, as well as artifact elimination [11];
- The **feature extraction and data analysis** steps consists of the choice and/or the definition of the features allowing a description of the informative signals. Further on, physiologically significant analysis must be made in order to provide medical interpretable results (see also [10]).

The third section will present our healthy volunteers data-

base, significantly enlarged since [10], and the results obtained by applying our abdominal sounds analysis toolbox to their recordings, taken in standardized conditions. We show that abdominal sound analysis detects trends in gastro-intestinal normal post-prandial activity and distinguishes among volunteers having different alimentary habits. In the fourth and last section, conclusion and future research directions are given.

Materials and methods

Our research is mainly methodological, so this section constitutes the core of this communication. As previously stated, it is organized in several subsections: signal acquisition/instrumentation, segmentation/denoising method, multi-channel processing and data analysis.

Data acquisition

Signal. Phonoenterograms are characterized by a succession of isolated and short events, clearly separated, whose frequency contents is relatively poor. They can appear in periodic bursts of activity (3 to 12 per minute, according to the place and time of their generation) [1, 2]. The literature indicates maximum frequencies of the abdominal sounds lower than 1000-1500 Hz. [4, 6, 12, 13], even if other values are mentioned (5000 Hz for example in [3]). The principal frequency of the abdominal sounds is generally higher than the frequencies of the cardiac and pulmonary sounds and sometimes a high-pass filtering at 80 Hz is used to eliminate their influence [4].

The literature description of the abdominal sounds is confirmed by our observations. The signal consists of a sparse succession of abdominal non-stationary impulsive sounds (figure 1). Its characteristics vary according to time, localization and patient. Its frequency contents is band-limited: only approximately 0.5% of the signal energy is located beyond 1000 Hz, and this percentage goes up to approximately 2% for frequencies between 500 - 2500 Hz, the phonoenterogram being energetic mainly between 100 and 500 Hz (figure 2). The parts of the signal which separate the sounds, called in the bibliography “periods of silence”, are not actually completely quiet. Noise due to acoustic effects of the stethoscope and to other low frequency physiological sounds (breathing, blood flow) is superimposed to the informative signal and must be taken into account in any further processing. Its frequency contents is almost identical to that of the signal and it cannot be eliminated by simple filtering.

Instrumentation. Most of the literature reports using classic microphones for acquiring abdominal sounds (as for example in [1, 2, 4, 12]). Recently, commercial electronic stethoscopes were used by Craine *et al.* [5, 6]. We have followed the approach of Garner et Ehrenreich [3], who adapt electret microphones to classic stethoscope heads, as it seems that it was the most appropriate solution to get auditive medical validation.

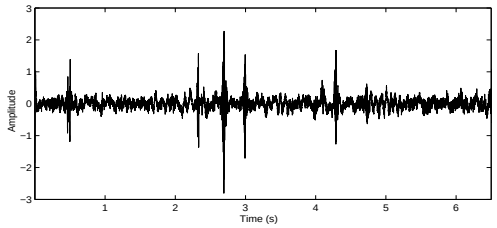

Figure 1: Example of 6.5 seconds of phonoenterogram

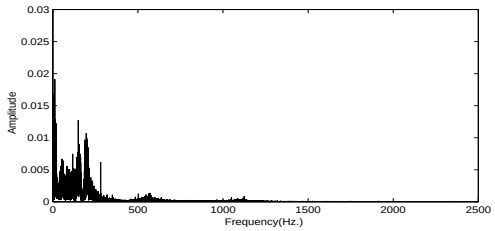

Figure 2: Typical phonoenterogram spectral contents

In fact, medical auscultation is performed by slightly pressing the stethoscope head towards the patient’s abdominal wall. It seems than important to estimate the influence of the stethoscope pressure on the recorded sound characteristics. Therefore, we estimated the frequency response of our sensor (microphone + stethoscope head) using a abdomen phantom towards which the stethoscope was pressed using different force values. As our goal was not to properly simulate bowel sounds but to asses pressure influence, the phantom we used was a lens-shaped balloon with adjustable surface tension. The sensor was pressed using calibrated weights, between 100 and 400 g, with a 50 g step. Measures were done in an anechoidal chamber, using a calibrated white noise source between 100 et 1000 Hz. As shown in figure 3, the frequency responses are very slightly influenced by the pressure and show a similar gain over the frequency band of interest. We concluded that the pressure does not significantly influence the abdominal sounds characteristics, so we could proceed with our recording campaign, knowing that comparison and analyze of different volunteers recordings were possible.

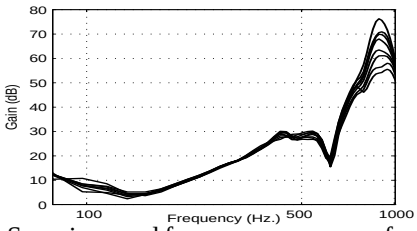

Figure 3: Superimposed frequency responses for different sensor pressures.

Acquisition protocol. Six-channels recordings were performed during 168 minutes, at a sampling frequency of 5 kHz, immediately following a standardized breakfast. The six stethoscopes were placed as in figure 4.

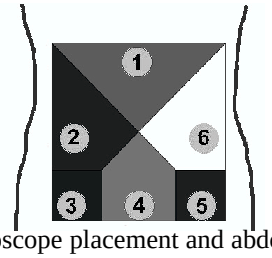

Figure 4: Stethoscope placement and abdominal regions.

Denoising and segmentation

Before interpretation, phonoenterograms must be denoised and segmented in individual sounds and, further on, parallel multi-channel acquisition must be taken into account for cross-validation and localization (as described in the next sub-section).

We have presented our denoising and segmentation technique in several communications before [8, 11], therefore we will only briefly remind it here and we will introduce a novel improvement, which better takes into account the impulsive nature of the abdominal sounds.

Iterative wavelet denoising. We consider the model $z = x + n$, where z is the given discrete–time signal to be denoised, x is the noise–free unknown version of z and n the noise. Orthogonal wavelet decomposition of z writes:

$$z = \sum_{p,j} w_z^{j,p}\ \psi^{j,p} + \sum_{p} w_z^{M,p}\ \phi^{M,p}, \qquad (1)$$

where j is the scale, p the position, ψ the wavelet, ϕ the scaling function and M the analysis depth [14].

Our denoising method develops the iterative wavelet–denoising method initially proposed by Starck and Bijaoui [15] and Coifman and Wickerhauser [16], applied by Hadjileontiadis *et al.* [17] to physiological sounds analysis. This method is particularly adapted to non-stationary transient extraction from stationary (but not necessarily Gaussian) noise [15, 17]. The denoised signal is estimated using an iterative scheme, yielding successive refinements of this signal: at each iteration, the largest wavelet coefficients of the residual noise contribute to the current estimate of the denoised signal.

In a previous work [8], we have shown that if no best basis procedure is considered (as in [16]), iterative denoising may be seen as a fixed-point algorithm determining independent thresholds for each scale. This interpretation leads to an important reduction of the computing burden as well as to a more rigorous way of parameterizing the algorithm. Moreover, in [11], we have analyzed and determined convergence conditions for this fixed-point method by introducing generalized Gaussian (GG) modelling of the wavelet coefficients. This approach leads to a "minimal" denoising algorithm, completely parameter-free and ensuring a maximum information extraction from the measured signal. The following paragraph briefly recalls these results.

Using the notations in eq. (1), the iterative denoising scheme originally proposed in [15–17] writes $z = \hat{x}_k + \hat{n}_k$, where k is the iteration step. The current noise estimation $\hat{n}_k$, initialized for $k = 0$ as $\hat{n}_0 = z$, is decomposed to obtain the noise coefficients vector $\Omega_{n,k}$. By thresholding $\Omega_{n,k}$, one obtains the current "peeled off layer" $\Omega_{\Delta x,k+1}$. The new noise coefficient vector $\Omega_{n,k+1}$ is obtained from $\Omega_{\Delta x,k+1} + \Omega_{n,k+1} = \Omega_{n,k}$.

The iterative threshold T_k computing method used for non–stationary transients detection in [15, 17] uses a classical ℓ_2 (outlier detection) criteria, based on the standard deviation σ_k of the noise coefficients vector $\Omega_{n,k}$ at iteration k. The fixed point descent algorithm writes [8]:

(1) compute σ_k as $(\sigma_k)^2 = \dfrac{1}{N}\ \sum_{p,j} \left(w_z^{j,p}\ g_{T_k}(w_z^{j,p})\right)^2$,

where $g_{T_k}(w_z^{j,p})$ are coefficients weights:

$$g_{T_k}(x) = \begin{cases} 1, & \text{if } |x| < T_k, \\ 0, & \text{if } |x| \geq T_k; \end{cases} \qquad (2)$$

(2) compute $T_{k+1} = F_a \sigma_k$ and loop till convergence.

This boils down to the following iterative relation:
$T_{k+1} = F_a \sqrt{\frac{1}{N}\sum_{p,j}\left(w_z^{j,p}\ g_{T_k}(w_z^{j,p})\right)^2}$.

Considering function f defined as

$$f(x) = F_a \sqrt{\frac{1}{N}\sum_{p,j}\left(w_z^{j,p}\ g_x(w_z^{j,p})\right)^2}, \qquad (3)$$

the final threshold is computed by the fixed-point descent algorithm $T_{k+1} = f(T_k)$. The values of the function f depend on the user constant F_a. For the bowel-sound denoising algorithm (WTST-NST) proposed by [17], the constant F_a equals 3, as in classical ℓ_2 outlier detection. Still, as we have shown in [8], F_a must be lower bounded in order to ensure the existence of a non null fixed point (*i.e.* denoising threshold), and 3 is not enough for heavy tailed distributions (*i.e.* very sparse signals, $u \lessapprox 0.8$). In [11], we have proposed a method for computing a lower bound for the multiplicative constant F_a. The wavelet coefficients are modelled by a generalized gaussian probability law:

$$p_{\sigma,u}(w) = \alpha e^{-|\beta w|^u} \ \text{ with} \qquad (4)$$

$$\beta = \frac{1}{\sigma}\sqrt{\frac{\Gamma(3/u)}{\Gamma(1/u)}},\ \alpha = \frac{\beta u}{2\Gamma(1/u)},\ \Gamma(u) = \int_0^\infty e^{-x}x^{u-1}dx,$$

where σ is the standard deviation and $u > 0$ is the shape parameter of the probability law (u=2 for a Gaussian and u=1 for the Laplace pdf).

Using this approach, we have shown that a sufficient condition for the fixed point algorithm convergence was $F_a \geq F_{am}$, with

$$F_{am} = \sqrt{\frac{3\beta}{2\alpha}(ue)^{\frac{1}{u}}} = \sqrt{\frac{3\Gamma(\frac{1}{u})}{u}(ue)^{\frac{1}{u}}}. \qquad (5)$$

The lower bound F_{am} is independent of σ and depends only on the shape u. As stated previously, a different $F_{am}(j)$ can be computed for each decomposition scale j.

As the F_{am} based threshold is generally lower than other classical or iterative thresholds [15, 17, 18], it ensures a maximum information extraction from the measured signal. Nevertheless, as a counterpart, the denoised estimate is generally noisier than the one obtained by other methods. In fact, the *universal threshold* $T_u = \sigma\sqrt{2\log N}$ (with σ the robust estimate of the noise standard deviation and N the length of the signal) proposed by Donoho and Johnstone [18] is the most widely used for denoising, as it leads to an almost completely noise-free *appearance* of the estimated informative signal. Still, the result of the universal thresholding is generally over-smoothed, and the mean-square error is often higher than the one obtained by other denoising algorithms (see Antoniadis *et al.* for a comparative review of a large number of wavelet denoising methods [19]).

Hysteresis thresholding. In this paragraph, we propose therefore an *ad hoc* method that combines universal thresholding and iterative denoising. The principle of the method is straightforward: as the signal of interest is a sparse succession of explosive transients, they will be more accurately detected and *segmented* by a high threshold, but a F_{am} iterative threshold will be used for *denoising* the segmented events. In other words, a high threshold will be used to eliminate all the noise between the informative events, and a maximum information will be extracted form these events by a low value threshold.

As the method for computing the low value threshold has already been described in the previous paragraph, we will propose here a way to obtain the high value threshold used for segmentation. In order to easily embed it in the iterative denoising algorithm, the multiplicative constant F_a in eq. (3) will be computed in order to initialize the threshold, if the estimated coefficients distribution is gaussian to the value of the universal threshold:

$$F_{ao} = \max(F_{am}, F_{ac}), \quad \text{with} \tag{6}$$

$$F_{ac} = K_c F_{am}, \quad \text{and} \quad K_c = \sqrt{\frac{2u\log N}{3\Gamma(\frac{1}{u})\sqrt{2e}}}. \tag{7}$$

One can easily check that $F_{ao} = F_{ac} = \sqrt{2\log N}$ for gaussian distributions ($u = 2$). The expression for F_{ao} (6) is justified by the fact that the value of K_c becomes smaller than 1 for very heavy-tailed distributions (shapes $u \lessapprox 0.4$), leading to an $F_{ac} \leq F_{am}$ and thus not ensuring the convergence of the fixed–point algorithm (figure 5).

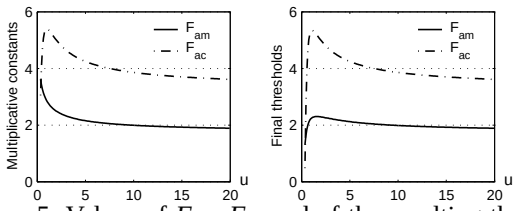

Figure 5: Values of F_{am}, F_{ac} and of the resulting thresholds for different shapes u. For the considered signals, the universal threshold $T_u \approx 4.99$.

Simulation results. In order to evaluate the performances of our method, we have considered a close-to-application simulated informative signal sampled at 5000 Hz and having 2^{18} samples (≈ 52 s). The signal was a series of short explosive events, randomly distributed in time, consisting on windowed sinusoids (hamming or decreasing exponential) having random frequencies (100 to 1000 Hz), random amplitudes (between 3 and 10) and random durations (20 ms to 1 s). We have considered 3 types of signal, with 5, 10 and 50 events.

Noise was added, generated according to 3 distributions: uniform ($u \to \infty$), Gaussian ($u = 2$) and Laplacian ($u = 1$), all three of them with 3 standard deviations ($\sigma = 0.5, 1, 2$). In a first test, the noise was left white. During a second test, it was filtered with a 8^{th} order finite response filter (FIR), chosen to provide a noise having a spectral contents close to the real abdominal signal.

We have compared 5 algorithms, using the classical mean square error criterion (MSE): our maximal thresholding (based on F_{ac}), our minimal thresholding (F_{am}), the resulting hysteresis thresholding, Hadjileontiadis' WTST-NST [17] and Donoho's universal hard-thresholding (*VisuShrink*) (table 1). Other classical denoising techniques (as *SureShrink* or *minimax*) are less adapted to sparse signals as they generally provide lower thresholds than *VisuShrink*.

Table 1: MSE for the 5 algorithms (mean values for all noise types and for different number of events signals).

Algorithm	Signal+white noise			Signal+colored noise		
	5 ev.	10 ev.	50 ev.	5 ev.	10 ev.	50 ev.
maximal	0.03	0.10	0.53	0.08	0.14	0.41
minimal	0.28	0.28	0.38	0.26	0.26	0.33
hysteresis	0.02	0.08	0.41	0.06	0.10	0.31
WTST-NST	0.10	0.13	0.28	0.10	0.12	0.25
VisuShrink	0.03	0.10	0.43	0.08	0.12	0.39

As seen in figure 5, our maximal threshold (used for event detection) is generally lower than the universal threshold (except for shapes $0.75 \lessapprox u \lessapprox 2.01$) and higher than the WTST-NST threshold (as $F_{ac} > 3, \forall u > 0.3$). This observation explains the results presented in table 1: the hysteresis threshold performs better than the others for sparse signals (when the maximal and the universal thresholds are too high and the minimal and WTST-NST are too low), but it falls behind WTST-NST (and even minimal, for white noise) when the events occur almost all along the simulated signal (50 events in 52 seconds). An example of denoising is presented figure 6 for a 10 events signal, with Laplacian white noise $\sigma = 1$.

Artifact elimination and multi-channel processing

Artifact elimination. Before proceeding to the multi-channel processing, we have decided to heuristically eliminate remaining artifacts, as no denoising method can ensure complete elimination of undesirable perturbations. In fact, noise cancelling methods deal with

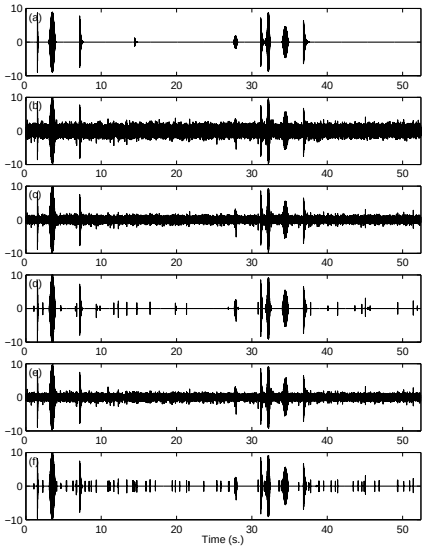

Figure 6: Denoising results: (a) original signal; (b) noisy signal; denoised signals using (c) minimal algorithm, (d) hysteresis algorithm, (e) WTST-NST, (f) *VisuShrink*. The denoised signal obtained by the maximal thresholding is not presented here, as it is visually similar to (d).

stationary noise, but non-informative (from a phonoenterographic point of view) signals ar not treated. Indeed, heart beats, patient movements, cough, are not eliminated by the wavelet denoising algorithm. We have introduced therefore *a priori* knowledge at this stage of our abdominal sound processing method. For each segmented event, we have computed the most popular physical features: the duration, the energy and the frequency spectrum, as in [4–6, 12]. Simple tests were done automatically on each event, and those who did not fit the literature description of an abdominal sound were eliminated: sounds having a duration smaller than 20 ms (like hair and skin friction on the stethoscope membrane) or larger than 1 second (movements), or having more than half of their energy below 80 Hz (like heart beats and respiration).

Multi-channel processing. There are two steps of multi-channel processing in our method (see figure 4 for stethoscope placement). The first one concerns artifact elimination by cross-validation. In fact, we assumed that real abdominal sounds propagate inside the abdomen. Therefore, we have eliminated all sounds that are not simultaneously acquired by at least two stethoscopes (that is, they are strictly not superimposed in time).

The second step is the localization technique. We have discussed different methods and we have proposed our approach in [9], so we will only briefly remind it here. In fact, very few publications present a multi-channel approach, and most of those who do it (like [4] for example) treat the recordings in a completely independent and parallel manner: they quantify abdominal sounds independently for each abdominal region and no propagation is taken into account. The only systematic approach was proposed by Craine *et al.* [6], who uses 3 stethoscopes to perform source localization by triangulation. As we have shown in [9], this approach is inaccurate, because of the high anisotropy of the propagation environment. Nevertheless, parallel recordings show differences in the abdominal sound activity, and sounds propagate inside the human body. The simplest hypothesis, and the most accurate for the moment, as long as no model of the abdomen is proposed, is that the recorded sounds are louder when the stethoscope is placed closer to their origin. Therefore, we have proposed a 6-region partition of the abdomen, as indicated figure 4. For each sound, we check its amplitude (acoustic intensity) on each of the stethoscopes that acquired it, and we place its origin inside the region indicated by the highest amplitude.

Feature extraction and data analysis

All the previously described steps of our phonoenterogram processing method can be considered as preprocessing steps. After localization, we have six noise and artifact-free signals, one for each abdominal region. For each signal, we have also the physical characteristics of the sounds that compose it: duration, energy, acoustic intensity, frequency. In the literature, several activity indices based on these physical features are proposed. We have identified nine of them, which we evaluated for each channel and for each minute of recording: the number of sounds (N_m), the total energy (E_m), the total duration of sounds in percents (D_m), the mean energy of sounds (E_μ), their mean duration (D_μ), their mean power (P_μ), their mean main frequency (f_μ), their mean acoustic intensity (I_μ) and the mean duration of silence periods between sounds ($D_{s,\mu}$). Each minute of recording can then be represented as a point in the nine-dimensional space obtained from the nine activity indices. Still, interpreting this information reveals to be difficult because of the high dimension of the representation space and, furthermore, because of the probable redundancy of the nine features. We have used principal component analysis (PCA) in order to analyze the dependencies between the above mentioned activity indices, eliminate redundancy and reduce the dimension of the representation space.

The PCA replaces the data (phonoenterograms minutes) in a new feature space. By ordering the variances of the new features, one can reduce the dimension of this new representation space. Correlations between the physical features (activity indexes) and PCA features can be used to assign physical interpretation to the latter. We have used a 4-dimensional features space, which keeps about 80% of the data variance (36%, 22%, 13% and 11% for c1, c2, c3 and c4 respectively). A rapid physical interpretation of the 4 retained principal components can be made as follows [10]: the signification of a new feature (principal component) is given by the most correlated physical feature (activity index). Using this technique, the first principal component c1 can be seen as a size variable, mainly correlated with energetic indices as E_m (0.73), P_μ (0.77), or I_μ (0.76), so we propose to interpret it as an activity level, or sound level measure. The second principal component c2 is correlated with time measures as D_m (0.71) or N_m (0.77), which suggest an interpreta-

tion as a measure of sound absence or sparsity. The third principal component c3 is related to the mean frequency f_μ (0.77))and can be interpreted as a pitch measure of the minute, while c4 is again a time measure, related to the mean duration of individual sounds D_μ (0.82).

The most common way of analyzing data in the PCA framework is to search for possible differences between predefined subgroups. We therefore group the phonoenterogram minutes either by abdominal region or by individual volunteer. In order to visualize these differences, the barycenter of each subgroup is projected onto the principal planes generated by the first 4 principal components c1-c4.

Experimental results

Our healthy volunteer data-base consists of 16 six-channel recordings having approximately 2 hours 48 minutes each (24 sequences of 2^{21} points per channel, at 5000 Hz sampling rate). We have therefore $16 \times 6 \times 168 = 16128$ minutes of phonoenterogram in our analysis database, which can be grouped, as described previously, by channel (abdominal region) or by patient. All the phonoenterograms were recorded in similar conditions, i.e. after a standardized breakfast taken at about 8:30 a.m. (a cup of tee/coffee, 2 bread rolls, 200 ml. of orange juice, 1 yoghurt). The volunteers were not allowed to change their position, which was halfway between lying and sitting, so they could watch television during the recording.

The results, obtained as described previously (projection of the barycenter on the principal planes) are promising (figures 7 and 8). Indeed, one can see that the third abdominal region (corresponding to the junction between the gut and the colon) is significantly more active than the others, both in terms of sound level (c1) and sparsity (c2) ($p \approx 0$ using a Wilcoxon test).

Another interesting result concerns the second patient (p2), which is different from the others. The most probable explanation is given by the alimentary habits of this volunteer: unlike the others, at the time of the recording he used to take dinner at about 1 o'clock in the morning, and he used to sleep at 8:30 (the recording hour). Usually, he didn't take any breakfast at all, the first meal being a normal lunch at about 1 p.m.

Conclusion and future research

In this communication, we have introduced a complete toolbox for phonoenterogram analysis. Several methodological steps were described and / or improved. Our phonoenterogram data-base is quite large and increasing (more than 16 000 minutes of recording by now), and the data analysis is at its first results, which seem promising. Further tests are in progress, in order to study the differences in time (evolution of the extracted features over the 3 hours of recording). For the moment, no pathologic case was recorded using the standardized protocol, but a shorter phonoenterogram of a patient with gastritis was easily distinguished from the others.

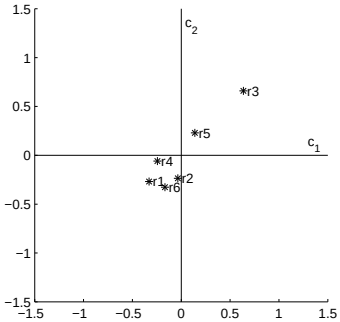

Figure 7: Means of the abdominal regions r1-r6 (see figure 4), projected on the principal plane c1-c2.

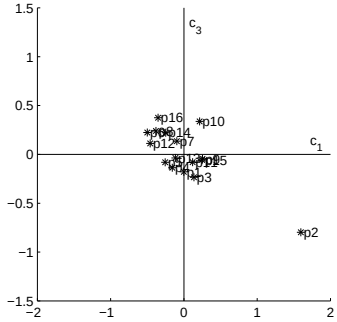

Figure 8: Means of the healthy volunteers p1-p16, projected on the principal plane c1-c3.

References

[1] CANNON, W. Auscultation of the rythmic sounds produced by the stomach and intestines. *Am. J. Physiology*, 14:339–353, 1905.

[2] FARRAR, J. and INGELFINGER, F. Gastrointestinal motility as revealed by study of abdominal sounds (with discussion). *Gastroenterology*, 29(5):789–802, 1955.

[3] GARNER, C. and EHRENREICH, H. Non invasive topographic analysis of intestinal activity in man on the basis of acoustic phenomena. *Res. Exp. Med. (Berl.)*, 189(2):129–140, 1989.

[4] TOMOMASA, T. *et al.* Gastrointestinal sounds and migrating motor complex in fasted humans. *Am. J. Roentgenology*, 94(2):374–381, 1999.

[5] CRAINE, B., SILPA, M., and O'TOOLE, C. Computerized auscultation applied to irritable bowel syndrome. *Digestive Diseases and Sciences*, 44(9):1887–1892, 1999.

[6] CRAINE, B., SILPA, M., and O'TOOLE, C. Two-dimensional positional mapping of gastrointestinal sounds in control and functional bowel syndrome patients. *Digestive Diseases and Sciences*, 47(6):1290–1296, 2002.

[7] YUKI, M. *et al.* Is a computerized bowel sound auscultation useful for the detection of increased bowel motility? *Am. J. Gastroenterology*, 97(7):1846–1848, 2002.

[8] RANTA, R., HEINRICH, C., LOUIS–DORR, V., and WOLF, D. Interpretation and improvement of an iterative wavelet–based denoising method. *IEEE Signal Processing Letters*, 10(8):239–241, 2003.

[9] RANTA, R., LOUIS–DORR, V., HEINRICH, C., WOLF, D., and GUILLEMIN, F. Towards an acoustic map of abdominal activity. In *Proceedings of IEEE-EMBS Conference*, Cancun, Mexico, September 2003.

[10] RANTA, R., LOUIS–DORR, V., HEINRICH, C., WOLF, D., and GUILLEMIN, F. Principal component analysis and interpretation of bowel sounds. In *Proceedings of IEEE-EMBS Conference*, San Francisco, USA, September 2004.

[11] RANTA, R., LOUIS–DORR, V., HEINRICH, C., and WOLF, D. Iterative wavelet–based denoising methods and robust outlier detection. *IEEE Signal Processing Letters*, 12(8):557–560, 2005.

[12] YOSHINO, H., ABE, Y., YOSHINO, T., and OHSATO, K. Clinical application of spectral analysis of bowel sounds in intestinal obstruction. *Dis. Col. Rectum*, 33(9):753–757, 1990.

[13] MANSY, H. and SANDLER, R. Detection and analysis of gastrointestinal sounds in normal and small bowel obstructed rats. *Med. Biol. Eng. Comput.*, 38(1):42–48, 2000.

[14] MALLAT, S. *A wavelet tour of signal processing*. Academic Press, 1999.

[15] STARCK, J.-L. and BIJAOUI, A. Filtering and deconvolution by the wavelet transform. *Signal Processing*, 35:195–211, 1994.

[16] COIFMAN, R. and WICKERHAUSER, M. Experiments with adapted wavelet de-noising for medical signals and images. In M. Akay, editor, *Time-Frequency and Wavelets in Biomedical Engineering*, pages 323–346. IEEE Press, 1998.

[17] HADJILEONTIADIS, L., LIATSOS, L., MAVROGIANNIS, C., ROKKAS, T., and PANAS, S. Enhancement of bowel sounds by wavelet-based filtering. *IEEE Transactions on Biomedical Engineering*, 47(7):876–886, 2000.

[18] DONOHO, D. and JOHNSTONE, I. Ideal spatial adaptation via wavelet shrinkage. *Biometrika*, 81:425–455, 1994.

[19] ANTONIADIS, A., BIGOT, J., and SAPATINAS, T. Wavelet estimators in nonparametric regression: a comparative simulation study. *Journal of Statistical Software*, 6(6):1–83, 2001.